

Studies of a Ka-band high power klystron amplifier at INFN-LNF

M Behtouei¹, B Spataro¹, L Faillace¹, A Leggieri², F Di Paolo², F Marrese², L Valletti², S Fantauzzi², G Torrisci³, M Carillo⁴, F Bosco⁴, A Mostacci^{1,4}, L Palumbo^{4,5} and M Migliorati^{4,5}

¹INFN-LNF, Via E. Fermi 40, Frascati, Italy

² Università degli Studi di Roma "Tor Vergata", Via del Politecnico, 1-00133-Roma, Italia

³ Istituto Nazionale di Fisica Nucleare (INFN/LNS) Lab. Nazionali del Sud, Catania, Italy

⁴ Department of SBAI, Sapienza University of Rome, Piazzale Aldo Moro 5, Rome, Italy

⁵ Istituto Nazionale di Fisica Nucleare (INFN-Roma1), Rome, Italy

E-mail: Mostafa.Behtouei@lnf.infn.it

Abstract. In the framework of the Compact Light XLS project [1], a Ka-band linearizer with electric field ranging from 100 to 150 MV/m is requested [2, 3, 4]. In order to feed this structure, a proper Ka-band high power klystron amplifier with a high efficiency is needed. This paper reports a possible solution for a klystron amplifier operating on the TM_{010} mode at 36 GHz, the third harmonic of the 12 GHz linac frequency, with an efficiency of 44% and 10.6 MW radiofrequency output power. We discuss also here the high-power DC gun with the related magnetic focusing system, the RF beam dynamics and finally the multiphysics analysis of a high- power microwave window for a Ka-band klystron providing 16 MW of peak power.

1. Introduction

Recent developments in accelerator science require higher power at higher frequencies. At the state of the art no stand-alone power sources can respond to these requirements, with the exception of systems composed by large combination of several power sources and pulse compression devices like SLEDs and corrugated waveguide structures.

In this paper we develop the design of a Ka-band klystron amplifier with an efficiency of 44% providing 10.6 MW radiofrequency output power. The paper is organized as follows: section 1 reports the electron gun injector design and magnetostatic simulation performed with CST Particle Studio [5], section 2 discusses the interaction structure which receives a beam current of 50 A and 480 kV with a beam radius of 1 mm confined in a drift tube of 1.2 mm radius. For the RF beam dynamics, the software KLyC [6] has been used. Much effort has been focused to obtain a sufficiently short structure suitable to accommodate a considerably narrow focusing magnet and to obtain the perveance needed for the required beam power output ensuring the maximum efficiency. In the section 3 we discuss the multiphysics analysis of a high- power microwave window for a Ka-band klystron providing 16 MW of peak power.

2. Electron gun injector design and magnetostatic simulation

The beam trajectory and the electric field equipotential lines are shown in figures 1a and 1b. The cathode-anodes geometry was optimized to adjust the electric field equipotential lines to



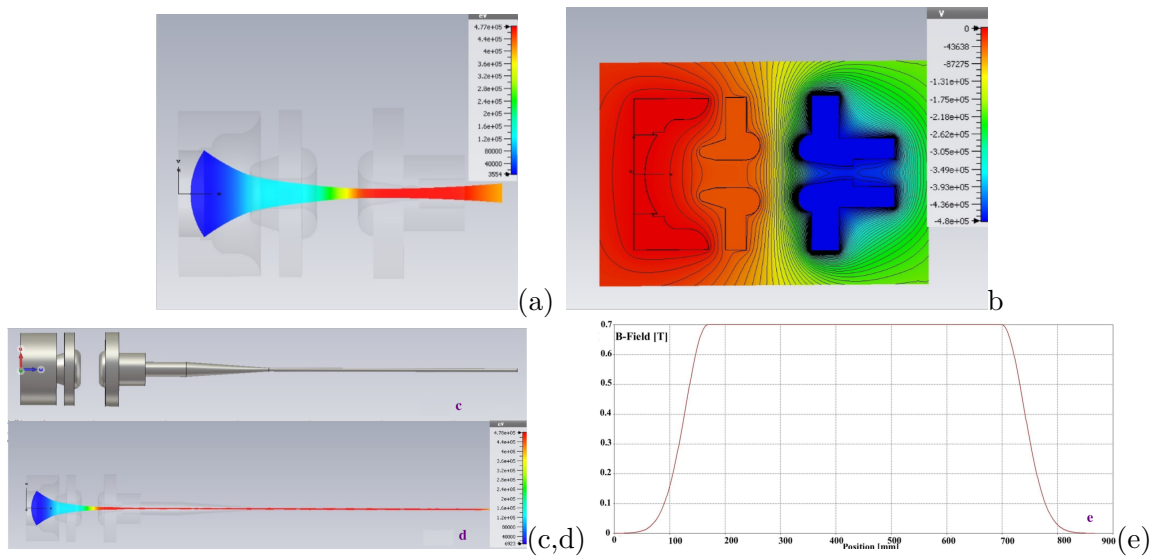


Figure 1. a) The dual anodes electron gun design from CST for a beam current of 50 A and the cathode-anode voltage of 480 kV. a) Beam trajectory b) equipotential lines c) 3D model of the gun d) beam trajectory along the propagation direction e) the axial magnetic field distribution.

obtain a beam current extraction of 50A. Figures 1c, d and 1e show the 3D model of the gun and of the beam pipe, the beam trajectory along the propagation direction and the axial magnetic field distribution, respectively.

The dual anode structure with an intermediate electrode allows us to overcome the strong space-charge force on the cathode and improve the transverse focusing [7], thus getting a low perveance. As a result, with this configuration, we are able to reduce the magnetic field value down to the normal conducting regime to confine the beam propagation in a pipe of 1.2 mm. This solution can be compared with our previous solution [8] using a magnetic focusing system working in superconducting regime. The magnetic field needed to compress the beam is reduced from 3.2 T to 0.7 T with this type of electron gun. The micro-perveance of this configuration is $0.15 \text{ AV}^{-3/2}$ which is a factor 2 less than the previous design [8]. The advantage of designing a low perveance electron gun is to get a weaker space charge, and, consequently, a stronger bunching. The maximum electric field on the focusing electrode is about 210 kV/cm almost the same of the previous configuration with standard anode. The design parameters of the gun with the focusing magnetic field along the beam axis for the beam current of 50 A are listed in table 1.

3. Interaction structure design

The numerical electromagnetic modeling has been set-up and performed based on the 1.5D large signal code KlyC [6] by adding the desired gain, bunch and output cavities. The layout of the interaction structure is shown in figure 2a.

Our proposed structure is composed by 9 cavities where the first three cavities and the fifth one operate in the first harmonic of the input signal while the fourth one operates on the second harmonic and the last four cavities are a system of coupled cavities operating at the third harmonic of the drive frequency ($f=12 \text{ GHz}$).

The cavity 4 is designed following the principle of the core oscillation method (COM) that is based on the non-monotonic bunching technique, where, along the length of the klystron, electrons at the periphery of the bunch gradually approach the bunch center. Simultaneously,

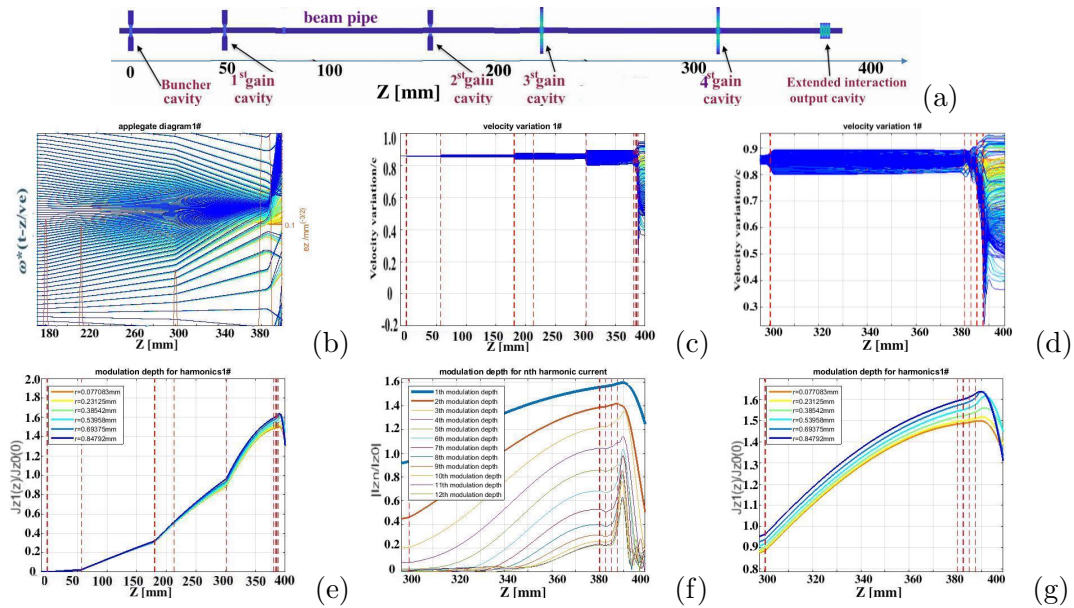


Figure 2. a) Layout of the interaction structure for the klystron with 50 A beam, b) the phase grouping, c and d) velocity variation of klystron with 50A, e) modulation depth of the 1^o harmonic current at different beam substrates f) modulation currents normalized to the DC current, J_{z0} as function of the longitudinal coordinate z and g) modulation depth of the 1st harmonic current.

Table 1. Design parameters of the gun with the focusing magnetic field along the beam axis.

Design parameters	
Beam power [MW]	24
Beam voltage [kV]	480
Beam current [A]	50
Micro-perveance [$I/V^{3/2}$]	0.15
Cathode diameter [mm]	45.5
Pulse duration, min-max range [μ s]	0.1- 0.2
Repetition rate [Hz]	10
Minimum beam radius in magnetic system [mm]	0.82
Nominal radius [mm]	0.925
Max EF on focusing electrode [kV/cm]	210
Electrostatic compression ratio	106:1
Beam compression ratio	697:1
Emission cathode current density [A/cm^2]	2.67
Transverse Emittance of the beam [mrad-cm]	0.63π

the core of the bunch experiences an oscillation in its phase, due to the space charge that causes it to expand, and the momentum delivered by successive bunching cavities that causes it to contract. The cavity RF fields have a weak effect on the periphery electrons (phase of $\pm\pi$ with respect to the core); as a result, COM klystrons require a substantial increase in their interaction length to capture all electrons in the bunch (a full saturated bunch) [9].

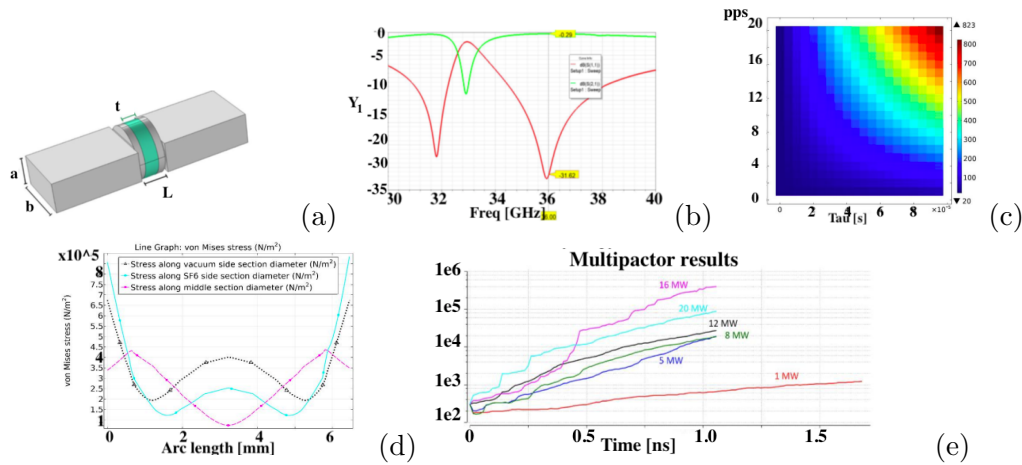


Figure 3. a) Pill-box window, b) scattering parameters of the pill-box window are plotted respect to the first propagating mode, c) steady state average Temperature (K) chart of the window, d) Von Mises Stress on the outer surfaces diameters and e) multipactor results.

The output circuit is an extended interaction output cavity that integrates four gaps. Extended interaction cavities can distribute the necessary retarding RF voltage at an output cavity over several gaps, thereby reducing the RF gradient and the danger of RF breakdown [9].

The phase grouping is shown in figure 2b. The electron beam has a considerably reduced energy, down to a velocity of $-0.09c$ along the z direction to achieve a high efficiency. The velocity variations are shown in figures 2c and 2d. In order to avoid reflected electrons, a minimal velocity, below $-0.1c$, has been considered in the output cavities.

The modulation depth of the 1st harmonic current at different beam substrates is shown in figure 2e. In this figure, J_{z1} is the 1st harmonic current normalized to the DC current, J_{z0} . The 1st harmonic content has a specific distribution on different substrates of the beam. It has been observed that, with respect to reentrant cavities, in pill-box cavities the gap electric fields for different radial positions exhibit reduced intensity spread. In order to exploit this feature and to have a reduced gain, needed for the last stage, the last gain cavity is a low R/Q pill-box cavity.

From figure 2f, it can be observed that the superior harmonic content grows while the signal is sufficiently compressed; this operation is demanded mostly to the last gain cavity. By observing the current distribution, the contribution to the superior harmonic content is mostly given by the inner part of the beam (the inner beam currents have the same behavior of harmonic currents), while the outer one behaves like the 1^o harmonic. Hence, the inner substrate of the beam should be richer in superior harmonic content and the outer beam substrate poorer (see figure 2g).

The output power of 10.6 MW and a total efficiency (considering losses) of 44% are obtained with an excellent minimal velocity around $0.2c$ that ensures no electron reflections and a maximum electric field less than about 134 kV/mm. The electric and geometric parameters of the proposed klystron are listed in table 2.

4. Design of a window for the Ka-band klystron

We presented a complete multiphysics design approach to design a window for the Ka-band klystron providing a peak power of 16MW [10] with an operating safety margin compared to 10.6 MW klystron output power. The proposed window is a pill-box type shown in figure 3a. The outer waveguides are WR28 type, while the inner one is a circular section where the ceramic window is brazed. After the optimization of the electromagnetic performances, we analyzed the effect of RF heating effect and the stress of the pressure on the window.

Table 2. Electric and geometric parameters of the proposed klystron.

CN*	HN**	F_0 [MHz]	R/Q [Ω]	M	Q_e	Q_{in}	z [mm]
1	1	12000	111	0.9597	30	4957	0.000
2	1	12038	111	0.9597	100000	4957	56.969
3	1	12250	111	0.9597	100000	4957	180.115
4	2	23790	27	0.8868	100000	1956	212.859
5	1	12095	33	0.9567	100000	2772	300.219
6	3	35255	117	0.6717	100000	4059	380.000
7	3	35255	117	0.6717	100000	4059	382.500
8	3	35255	117	0.6717	100000	4059	385.000
9	3	35255	117	0.6717	47	4059	387.500

* Cavity number.

** Harmonic number.

The scattering parameters of the pill-box window are shown in figure 3b. In figure 3c we demonstrated that the average temperatures reached by the window depend on pulse per second (pps) and pulse width (τ) with 16 MW of peak power, with operational mode TE₁₀-TE₁₁. Figure 3d shows the stress along the diameters of the vacuum-side, air-side surfaces and of the middle section of the cylindrical window. Multipactor problems have also been analyzed (see figure 3e) and mitigated, since this phenomenon is often cause of window failures.

The design reported in this work shows that the microwave window stimulated by a pulse of 200 ns and 16 MW of peak power does not show a significant increase in temperature and it is possible to avoid the harmful phenomenon of multipactor by TiN Coating of the microwave window.

5. Conclusion

In this paper, we presented a design of a low perveance dual anode electron gun for a high efficiency klystron in order to feed a phase space linearizer operating on the third harmonic of the main linac frequency. The simulation has been carried out with CST Particle Studio. The RF beam dynamics has been discussed for this configuration. Finally a multiphysics design approach has been considered for a window of a Ka-Band klystron providing 16 MW of peak power.

Acknowledgements

This work was partially supported by the Compact Light XLS Project, funded by the European Union's Horizon 2020 research and innovation program under grant agreement No. 777431 and was also partially funded by ARYA and MICRON projects of the Vth Committee of the INFN.

References

- [1] D'Auria G, Cross A, Zhang L and Nix L 2021 Conceptual Design Report of the CompactLight X-ray FEL
- [2] Behtouei M, Faillace L, Ferrario M, Spataro B and Variola A 2020 *J. Phys.: Conf. Series* **1596** 012021
- [3] Spataro B, Behtouei M, Faillace L, Variola A, Dolgashev V, Rosenzweig J, Torrisi G and Migliorati M 2021 *Nucl. Instrum. Methods Phys. Res., Sect. A* **1013** 165643
- [4] Behtouei M, Faillace L, Spataro B, Variola A and Migliorati M 2020 *Nucl. Instrum. Methods Phys. Res., Sect. A* **984** 164653
- [5] 2020 CST Studio Suite solvers, electromagnetic simulation and compatibility, cad
- [6] Cai J and Syratchev I 2019 *IEEE Trans. Plasma Sci.* **47** 1734–41
- [7] Shang F, Shang L and Li J 2016 The measurement system of the electron gun with double-anode structure *Proc. 7th Int. Particle Accelerator Conf. (IPAC'16)* (Busan, Korea) pp 3954–6

- [8] Behtouei M, Spataro B, Di Paolo F and Leggieri A 2021 *Vacuum* **191** 110377
- [9] Caryotakis G 2004 High Power Klystrons: Theory and Practice at the Stanford Linear Accelerator CenterPart I Tech. rep. SLAC National Accelerator Laboratory, Menlo Park, CA, USA
- [10] Marrese F, Valletti L, Fantauzzi S, Leggieri A, Behtouei M, Spataro B and Di Paolo F 2022 *JOMe* **21** 157–70